A Family of Metal–Organic Frameworks Based on Carboxylates and a Neutral, Long, and Rigid Ligand: Their Structural Revelation, Magnetic, and Luminescent Property Study

ARTICLE *in* CRYSTAL GROWTH & DESIGN · NOVEMBER 2013

Impact Factor: 4.89 · DOI: 10.1021/cg401403a

4 AUTHORS, INCLUDING:

Sanda Suresh
Indian Institute of Science Education and Res…
17 PUBLICATIONS **133** CITATIONS
SEE PROFILE

Srinivasulu Parshamoni
Indian Institute of Science Education and Res…
15 PUBLICATIONS **97** CITATIONS
SEE PROFILE

Amit Adhikary
Missouri University of Science and Technology
20 PUBLICATIONS **264** CITATIONS
SEE PROFILE

CRYSTAL GROWTH & DESIGN

Article

pubs.acs.org/crystal

A Family of Metal–Organic Frameworks Based on Carboxylates and a Neutral, Long, and Rigid Ligand: Their Structural Revelation, Magnetic, and Luminescent Property Study

Suresh Sanda,[†,‡] Srinivasulu Parshamoni,[†,‡] Amit Adhikary,[†] and Sanjit Konar*[,†]

[†]Department of Chemistry, IISER Bhopal, Bhopal 462023, India

Supporting Information

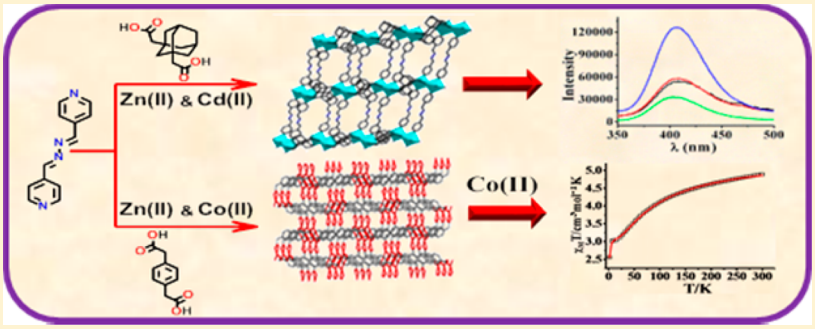

ABSTRACT: Four new two-dimensional/three-dimensional (2D/3D) bpmh-based metal organic frameworks, namely, $\{[Zn(1,3\text{-adaa})(bpmh)]\}_n$ (**1**), $\{[Cd(1,3\text{-adaa})(bpmh)]\}_n$ (**2**), $\{[Zn(1,4\text{-pdaa})(bpmh)]\}_n$ (**3**), and $\{[Co(1,4\text{-pdaa})(bpmh)]\}_n$ (**4**) (bpmh = *N*,*N*-bis-pyridin-4-ylmethylene-hydrazine, 1,3-adaa = 1,3-adamantane diacetic acid, 1,4-pdaa = 1,4-phenylene diacetic acid) have been synthesized through the slow diffusion technique. Structural determination reveals that compounds **1** and **2** have 2D layered architectures with similar framework topology, whereas **3** and **4** are isostuctural 3D frameworks. Both **1** and **2** perceives a common secondary building unit (SBU) $[M_2(adaa)_4(bpmh)_4]$ [M = Zn(**1**) and Cd(**2**)]. In compound **1**, 1,3-adaa exhibits both μ- 1,1 and μ- 1,2 bridging modes, whereas in **2** it shows both μ-1,1 and μ-1,1,2 bridging modes. The difference in the bridging mode of 1,3-adaa in **1** (Zn) and **2** (Cd) is responsible for the shorter M···M contacts in **2** (3.872 Å) than in **1** (4.13 Å) in the SBU. The 1,3-adaa ligands are sandwiched between the bpmh linkers in compounds **1** and **2.** In compounds **3** and **4**, 1,4-pdaa exhibits both μ-1 and μ-1,1 bridging modes and are isostructural in nature. The metal centers are arranged in a helical fashion around 2_1 screw axis in **3** and **4**. In compounds **1**–**4**, the used dicarboxylic acids act as pillars between the metal-bpmh layers. Solid-state photoluminescent properties of compounds **1**–**3** show ligand ($n \rightarrow \pi^*$ and $\pi \rightarrow \pi^*$)-based florescence. The magnetic studies of compound **4** show presence of the antiferromagnetic exchange between the metal centers.

INTRODUCTION

Over the past few decades, metal–organic frameworks (MOFs) have attracted immense attention of the scientists because of their versatile structural features such as large surface area,[1] porous structures,[2] and potential applications in sensing,[3] catalysis,[4] magnetism,[5] drug delivery, etc.[6] The current research interest in luminescent MOFs stems from their potential applications as molecular sensors,[7] in light-emitting diodes,[8] and detection of explosives.[9] In this context, using π-conjugated, rigid organic linkers is an effective approach to synthesize luminescent MOFs where luminescence is based on the ligand.[8b]

In a broad sense, MOFs contain two central components, connectors, and linkers. Connectors (can also be secondary building units or SBUs) are mostly metal centers and linkers are organic molecules.[10] Linkers afford a wide variety of linking sites with tuned binding strength, directionality, and flexibility. Long flexible ligands generally yield flexible frameworks, and as a host, these are typically guest responsive. But the major problem of long flexible ligands is their tendency to form an interdigitated scaffold, and once the frameworks are formed their stability and recurring behavior toward guests could be a point of concern. So, rigid ligands are more preferable in these circumstances. Some of the neutral, rigid bridging ligands like pyrazine,[11] 4,4′-bipy,[12] and 4,4′-azobis(pyridine)[13] have been used extensively in combination with mono and dicarboxylate ligands to synthesize MOFs. In this work, we have prepared a neutral, long, and rigid bis-pyridyl ligand and that has been used to synthesize two quasi isostructural 2D frameworks and two isostructural 3D frameworks in combination with two different dicarboxylic acids. Compounds **1**–**3** reveal ligand-based photoluminescence properties in the solid state. The magnetic properties of compound **4** show antiferromagnetic behavior among the metal centers.

Received: September 21, 2013
Revised: October 30, 2013

   dx.doi.org/10.1021/cg401403a | *Cryst. Growth Des.* XXXX, XXX, XXX–XXX

Table 1. Crystallographic Data for 1−4

	1	2	3	4
empirical formula	$C_{26}H_{28}N_4O_4Zn$	$C_{26}H_{28}N_4O_4Cd$	$C_{22}H_{18}N_4O_4Zn$	$C_{22}H_{18}N_4O_4Co$
chemical formula weight	525.91	572.93	467.79	461.19
crystal shape	block	block	block	block
color	yellow	yellow	yellow	pink
size (mm)	0.42 × 0.35 × 0.28	0.42 × 0.38 × 0.27	0.42 × 0.36 × 0.25	0.43 × 0.35 × 0.25
crystal system	triclinic	triclinic	monoclinic	monoclinic
space group	$P\bar{1}$	$P\bar{1}$	$P2_1/c$	$P2_1/c$
a (Å)	9.804(2)	9.2841(11)	10.2678(8)	10.327(3)
b (Å)	10.291(3)	10.7513(13)	13.0131(10)	12.999(4)
c (Å)	12.584(3)	13.1913(15)	15.9584(11)	15.985(5)
α (deg)	80.787(11)	75.121(5)	90.00	90.00
β (deg)	68.059(10)	73.020(5)	110.229(5)	110.367(19)
γ (deg)	84.556(12)	83.385(5)	90.00	90.00
cell volume, V (Å^3)	1161.6(5) Å^3	1215.9(2) Å^3	2000.8(3) Å^3	2011.7(11) Å^3
cell formula units Z	2	2	4	4
wavelength (Mo Kα)	0.71073	0.71073	0.71073	0.71073
temperature (K)	296(2)	296(2)	296(2)	296(2)
theta range for data collection	2.82 to 28.44	2.30 to 35.31	5.66 to 28.31	3.13 to 23.15
goodness-of-fit	1.147	1.064	1.066	1.074
R_{factor} all	0.0511	0.0306	0.0437	0.0944
wR_2	0.1631	0.0948	0.1084	0.2161
F(000)	548.0	584	960	948

EXPERIMENTAL SECTION

Materials. All the reagents and solvents for synthesis were purchased from commercial sources and used as supplied without further purification. All the metal salts, 1,3-adamantane diacetic acid, 1,4-phenylene diacetic acid, and pyridene-4-aldehyde were obtained from the Sigma-Aldrich chemical company.

Physical Measurements. Thermogravimetric analysis was recorded on a Perkin-Elmer TGA 4000 instrument. IR spectrum of the compounds **1**−**4** were recorded on a Perkin-Elmer FT-IR Spectrum BX using the KBr pellets in the region of 4000−400 cm^{-1}. Elemental analysis was carried out on a Elementar vario Micro Cube Elemental Analyzer. PXRD patterns were measured on a PAnalytical Empyrian instrument by using Cu Kα radiation. All the solid-state fluorescence measurements were recorded on a Horiba Jobin−Yvon Fluorolog3 instrument. Magnetic measurements were performed using a Quantum Design SQUID-VSM magnetometer. The measured values were corrected for the experimentally measured contribution of the sample holder, while the derived susceptibilities were corrected for the diamagnetism of the samples, estimated from Pascal's tables.[14]

Single Crystal X-ray Diffraction. Single crystal data for compounds **1**−**4** were collected on a Bruker APEX II diffractometer equipped with a graphite monochromator and Mo Kα (λ = 0.71073 Å, 296 K) radiation. Data collection was performed using the φ and ω scans. The structures were solved using direct method followed by full matrix least-squares refinements against F^2 (all data HKLF 4 format) using SHELXTL.[15] Subsequent difference Fourier synthesis and least-squares refinement revealed the positions of the remaining non-hydrogen atoms. Determinations of the crystal system, orientation matrix, and cell dimensions were performed according to the established procedures. Lorentz polarization and multiscan absorption correction were applied. Nonhydrogen atoms were refined with independent anisotropic displacement parameters, and hydrogen atoms were placed geometrically and refined using the riding model. All calculations were carried out using SHELXL 97,[16] PLATON 99,[17] and WinGXsystemVer-1.64.[18] Data collection and structure refinement parameters and crystallographic data for the complexes **1**−**4** are given in Table 1. Selected bond lengths and bond angles for compounds **1**−**4** are given in Table S1 of the Supporting Information.

*Synthesis of {[Zn(1,3-adaa)(bpmh)]}$_n$ (**1**).* bpmh was synthesized by the literature procedure.[19] An aqueous solution of (5 mL) Na salt of 1,3-adaa (0.05 mmol, 14.8 mg) was mixed stepwise with ethanol solution (5 mL) of bpmh (0.05 mmol, 10.5 mg) while being stirred, and the resulting solution was further stirred for 30 min to mix well. $Zn(NO_3)_2{\cdot}6H_2O$ (0.1 mmol, 29.7 mg) was dissolved in 10 mL of water and put in a narrow tube. Two milliliters of the above-mixed ligand solution was slowly and carefully layered over 2 mL of this metal solution. X-ray quality yellow-colored rectangular-shaped single crystals were obtained from the junction of the layer after 7 days. The crystals were separated and washed with ethanol and air-dried (yield = 40% based on metal). Elemental analysis, Anal. Calcd: C, 59.38%; H, 5.37%; N, 10.65%. Found: C, 60.5%; H, 4.9%; N, 10.5%. FT-IR (KBr pellet, cm^{-1}) 3435(br), 2899(w), 2518(w), 1615(w), 1516(w), 1535(s), 1426(br), 1200(m), 1123(s), 1098(w).

*Synthesis of {[Cd(1,3-adaa)(bpmh)]}$_n$ (**2**).* The same diffusion technique of **1** was employed for the synthesis of compound **2** using the $CdCl_2$, bpmh, and 1,3-adaa in a 1:0.5:0.5 molar ratio, using methanol as a solvent instead of ethanol. Yield (30% based on metal) elemental analysis, Anal. Calcd: C, 54.51%; H, 4.93%; N, 9.78%. Found: C, 55.30%; H, 5.40%; N, 9.20%. FT-IR (KBr pellet cm^{-1}) 3424(br), 1636(m), 1607(s), 1434(s), 1309(w), 1239(w), 1009(w).

*Synthesis of {[Zn(1,4-pdaa)(bpmh)]}$_n$ (**3**).* An aqueous solution of (10 mL) Na salt of 1,4-pdaa (0.1 mmol, 23.8 mg) was mixed in parts with methanol solution (10 mL) of bpmh (0.1 mmol, 21 mg) while stirring, and the resulting solution was further stirred for 1 h to mix well. $Zn(NO_3)_2{\cdot}6H_2O$ (0.1 mmol, 29.7 mg) was dissolved in 10 mL of water and put in a narrow tube. Two milliliters of the above mixed ligand solution was slowly and carefully layered over 2 mL of this metal solution.

X-ray quality dark-yellow-colored block-shaped single crystals were obtained from the junction of the layer after 3 days. The crystals were separated and washed with MeOH and air-dried (yield = 35% based on metal). Elemental analysis, Anal. Calcd: C, 56.49%; H, 3.88%; N, 11.98%. Found: C, 55.80%; H, 3.5%; N, 12.1%. FT-IR (KBr pellet cm^{-1}) 3154(b), 1610(s), 1550(s), 1420(w), 1387(s), 1306(m), 1237(w), 1161(w), 1063(w).

*Synthesis of {[Co(1,4-pdaa)(bpmh)]}$_n$ (**4**).* The same diffusion technique of **3** was employed for the synthesis of compound **4** using the $Co(NO_3)_2{\cdot}6H_2O$, bpmh, 1,4-pdaa in 1:1:1 molar ratio, X-ray quality pink-colored, block-shaped single crystals were obtained after 3 days. The crystals were separated and washed with MeOH and air-dried (yield = 40%). Elemental analysis, Anal. Calcd: C, 57.28%; H,

dx.doi.org/10.1021/cg401403a | Cryst. Growth Des. XXXX, XXX, XXX−XXX

3.93%; N, 12.14%. Found: C, 56.4%; H, 3.5%; N, 12.5%. FT-IR (KBr pellet cm^{-1}) 3415(b), 1610(m), 1549(s), 1420(w), 1387(s), 1306(m), 1237(w), 1161(w).

RESULTS AND DISCUSSION

Synthetic Aspects. Usage of highly conjugated ligands for the synthesis is an effective way to prepare luminescent MOFs. Few MOFs are reported (Table S2 of the Supporting Information) by using bpmh linker in combination with other dicarboxylic acids.[20] Although it is a highly conjugated and rigid ligand, very few reports are available in the literature on luminescence properties of MOFs where bpmh is one of the organic linker.[20a−c] In this aspect, we choose bpmh linker in combination with the V-shaped 1,3-adaa ligand (Scheme 1) and

Scheme 1. Ligands Used for This Work

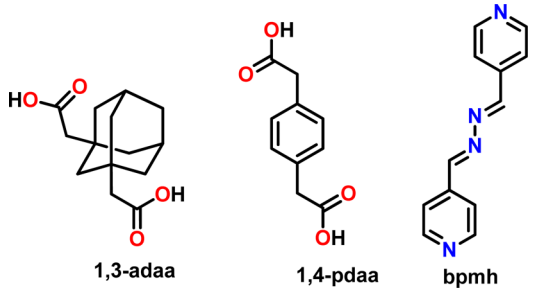

we have synthesized two 2D MOF's by using Zn(II) and Cd(II) metal atoms because metal ions with d^{10} configuration show intriguing fluorescent behavior. On the other hand, we changed the 1,3-adaa ligand with 1,4-pdaa to synthesize compounds **3** and **4** (Scheme 2).

Although the same diffusion technique was followed to prepare all the compounds, the dimensionality of the frameworks have been changed in compounds **3** and **4** and might be due to the flexible nature of the 1,4-pdaa ligand. The powder XRD of **1**−**4** (Figures S1 and S2 of the Supporting Information) are in very good correspondence with the simulated patterns of the single crystal, indicating the phase purity of bulk samples. The purity of the samples was further confirmed by IR spectra (Figures S3−S6 of the Supporting Information) and elemental analysis.

Structural Description of {[Zn(1,3-adaa)(bpmh)]}n (1). Single-crystal X-ray structure determination reveals that compound **1** crystallizes in the triclinic $P\bar{1}$ space group and is a neutral two-dimensional framework. The asymmetric unit contains a Zn(II) atom, one 1,3-adaa ligand, and one bpmh linker (Figure S7 of the Supporting Information). Here, each Zn(II) center adopts a distorted octahedral geometry with the ZnO_4N_2 coordination environment (Figure 1). Each Zn(II)

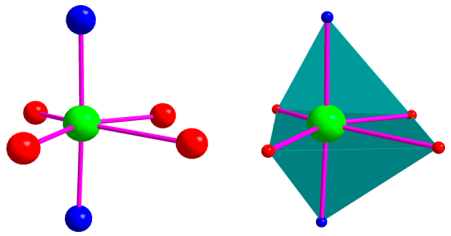

Figure 1. Octahedral coordination environment around Zn(II) atom in compound **1**. Color code: oxygen (red), nitrogen (blue), and zinc (green).

ligated to the four oxygen atoms of 1,3-adaa, which occupy the equatorial positions [Zn−O bond lengths are in the range of 2.015(3)−2.393(3) Å], and the axial sites are occupied by two nitrogen atoms of bpmh linker [bond lengths of Zn1−N1 and Zn1−N4 are 2.196(2) Å and 2.190(3) Å].

Compound **1** contains a repeated $[Zn_2(adaa)_4(bpmh)_4]$ unit and can be considered as secondary building units (SBUs), which are connected through the V-shaped carboxylate groups of 1,3-adaa ligands and forms the 1D chain along the *a* axis (Figure 2). The angle between the two carboxylate groups in

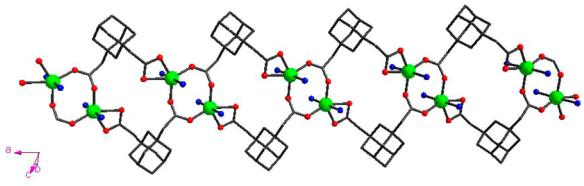

Figure 2. 1D Chain of compound **1** along the *a* axis. Color code is the same as in Figure 1.

the 1,3-adaa ligand is 93.69°. Further, the 1D chain extended through the bpmh linkers in the axial position along the crystallographic *b* axis and results in a 2D layer in the *ac* plane (Figure 3). The distance between two Zn(II) centers in the

Scheme 2. Synthetic Details of All the Compounds Reported in This Paper

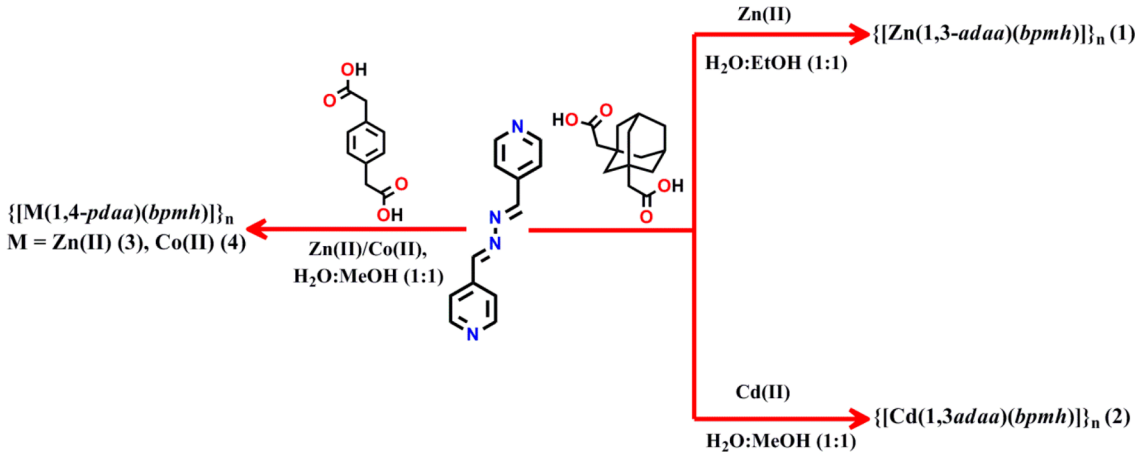

dx.doi.org/10.1021/cg401403a | Cryst. Growth Des. XXXX, XXX, XXX−XXX

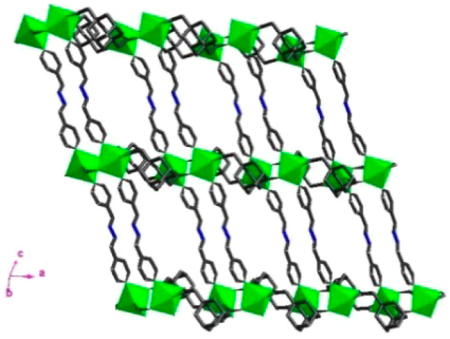

Figure 3. 2D Framework of compound **1**. coordination environment around Zn atom is shown as green polyhedra. Color code: C−C (gray) and N−N (blue).

SBU is 4.13 Å and between two SBU units bridged by the 1,3-adaa ligand is 7.510 Å. Each 1,3-adaa connects three Zn(II) atoms in two different bridging modes (μ-1,1 and μ-1,2) (Figure S8 of the Supporting Information), whereas each bpmh linker holds two Zn(II) at a distance of 15.860 Å. The angle between the O1−Zn1−O2 in the μ-1,1 mode is 57.81°. The schematic representation of zinc centers bridged by 1,3-adaa and bpmh in the 2D framework is represented in Figure S9 of the Supporting Information. It has been noted that 1,3-adaa ligands are sandwiched alternatively between the bpmh ligands down the *c* axis, as shown in Figure S10 of the Supporting Information.

*Structural Description of {[Cd(1,3-adaa)(bpmh)]}$_n$ (**2**).* Compound **2** crystallizes in same $P\bar{1}$ space group having similar framework topology like **1**, but they are not isostructural. The coordination diversities of the 1,3-adaa ligand induce hepta coordination environment around the Cd(II) centers. The asymmetric unit contains one Cd(II) atom, one 1,3-adaa ligand, and the bpmh linker (Figure S11 of the Supporting Information). Here, each hepta-coordinated Cd(II) ion with a CdO_4N_2 coordination environment shows nearly pentagonal bipyramidal geometry (Figure 4).

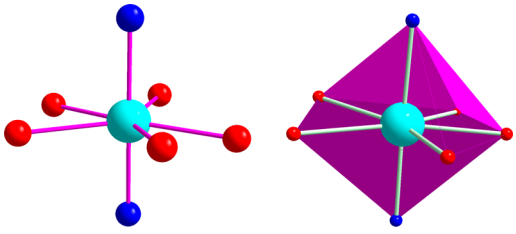

Figure 4. Pentagonal bipyramidal arrangement of Cd(II) atom in compound **2**. Color code: oxygen (red), nitrogen (blue), and cadmium (turquoise).

The hepta coordination environment around the Cd(II) center fulfilled by five oxygen atoms from three different 1,3-adaa ligands at the equatorial positions [Cd−O bond lengths are in the range of 2.345(2) Å−2.492(3) Å] and two nitrogen atoms from two different bpmh linkers at the axial positions [bond lengths of Cd−N1 and Cd1−N2 are 2.334(2) Å and 2.320(2) Å, respectively]. Compound **2** also contains SBU ($[Cd_2(adaa)_4(bpmh)_4]$ units), which are repeated along the 1D chain formed by interconnection of the units through the carboxylate group of the 1,3-adaa ligand (Figure S12 of the Supporting Information). The angle between the two carboxylate groups in 1,3-adaa is shorter by 6.01° (87.68°), in comparison to compound **1**. Further, the 1D coordination chain extends through the bpmh linkers along the crystallographic *b* axis and formed a 2D layer in the *ac* plane (Figure 5).

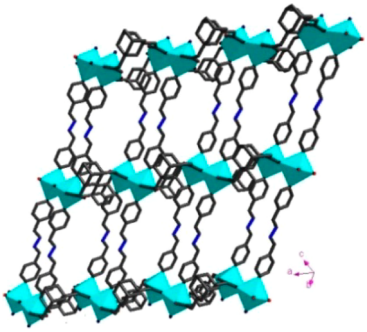

Figure 5. 2D-Layered structure of compound **2.** Coordination environment around the Cd atom is shown as polyhedra (turquoise). Color code is the same as in Figure 3.

The distance between two Cd(II) centers bridged by the 1,3-adaa ligand in the 1D chain is 6.714 Å, which is marginally shorter than that found in **1**. In **2**, each 1,3-adaa coordinated to the metal centers through μ-1,1- and μ-1,1,2-bridging modes and each bpmh bridges two Cd(II) centers having a distance of 15.951 Å. Out of five oxygen atoms around each Cd(II) center, two oxygen atoms from two different 1,3-adaa ligands coordinated through μ-fashion and form a carboxy-O bridge between two Cd(II) centers, resulting in a centro symmetric dimer (Figure S13 of the Supporting Information). The noted bridging mode of the carboxy group of the 1,3-adaa ligand consequence a shorter Cd···Cd distance (3.872 Å) within the SBU in comparison to the Zn···Zn distance found in compound **1**. The angle around the centrosymmetric dimer are O2−Cd1−O2A = 69.84(7)° and Cd1−O2−Cd1A = 110.16(8)°. From the structural comparison between **1** and **2**, it can be concluded that the coordination diversities of 1,3-adaa results in the centrosymetric Cd(II) dimer in **2** and also induces shorter intra-chain Cd(II)···Cd(II) separation. The schematic representation of the cadmium centers bridged by 1,3-adaa and bpmh in the 2D framework is represented in Figure S14 of the Supporting Information.

Notably, noncovalent interactions such as localized [C61−H61···C24 = 3.582(4) Å] and semilocalized C−H···π (C9−H9···C16/C19 = 3.380 Å), C−H···O [C21−H21···O3 = 3.146(4) Å and C21−H21···O1 = 3.116(3) Å] are perceived between the two ligands, which assists the formation of the above 2D framework. A face-to-face π···π interaction (3.782 Å) between the neutral bpmh ligand along the *c* axis is observed, which further stabilizes the 2D framework. As noticed in **1**, in **2**, 1,3-adaa ligands are also sandwiched in between the bpmh ligands down the *c* axis, as shown in Figure S15 of the Supporting Information.

*Structural Description of {[Zn(1,4-pdaa)(bpmh)]}$_n$ (**3**) and {[Co(1,4-pdaa)(bpmh)]}$_n$ (**4**).* Structural investigation reveals that compounds **3** and **4** crystallize in the monoclinic $P2_1/c$ space group. The asymmetric unit comprises one metal atom, one 1,4-pdaa ligand, and one bpmh linker (Figure S16 of the Supporting Information). Each metal atom is connected to three 1,4-pdaa ligands through two μ-1 and one μ-1,1 carboxylate oxygens and two nitrogen atoms from the bpmh linkers. Similar to compounds **1** and **2**, in **3** and **4** the 1,4-pdaa

dx.doi.org/10.1021/cg401403a | *Cryst. Growth Des.* XXXX, XXX, XXX−XXX

ligands are situated on the equatorial position [the M−O bond lengths are in the range of 2.0479(2)−2.298(2)Å in Zn(II) and 1.997(5)−2.236(4) Å in Co(II)], whereas the neutral bpmh ligand in the axial position [M−N bond lengths are in 2.151(2) and 2.156(2) Å in Zn(II) and 2.172(4) Å and 2.191(6) Å in Co(II)], resulting in a distorted octahedral geometry around the metal center. Compounds **3** and **4** contain a similar SBU {[M_2(pdaa)$_4$(bpmh)$_4$ units], where M = Zn(**3**) and Co(**4**)} as observed earlier. The distance between the two metal centers in the SBU is 3.996(2) Å in **3** and 4.052(1) Å in **4**. The metal centers in one SBU are bridged to six other SBUs by two μ-1,1 1,4-pdaa ligands and two neutral bpmh ligands. The distance between the metal centers bridged by the 1,4-pdaa ligand is the same in both compounds [8.449 (3) Å] and by the bpmh ligand is 15.709(3) Å in Zn(II) and 15.725(5)Å in Co(II) respectively.

It is interesting to note that each bpmh ligand bridged to the SBUs and extended along the *c* axis to form a 1D coordination polymer. Throughout the 1D chain, bpmh ligands exhibit parallel displaced $\pi\cdots\pi$ interactions of 3.971 Å; due to this, metal centers are arranged in helical fashion around the 2_1 screw axis (Figure S17 of the Supporting Information). These 1D chains are interconnected through the carboxylate groups of 1,4-pdaa ligands in the equatorial positions to form a 2D layer in the *bc* plane (Figure 6), and these layers are further pillered by the other carboxylate group of 1,4-pdaa ligand to generate the 3D framework (Figure 7).

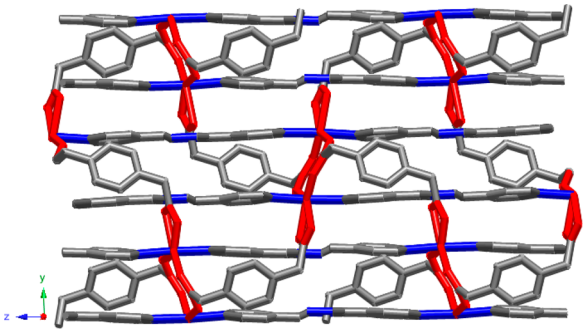

Figure 6. 2D Layer of compounds **3** and **4** in the *bc* plane. Color code: M−O (red), M−N (blue), and C−C (gray).

Thermal and PXRD Analysis. To investigate the thermal stability of compounds **1**−**4**, thermogravimetric analysis (TGA) was carried out in the temperature range of 30−650 °C under a flow of N_2 with a heating rate of 10 °C min^{-1} (Figure S18 of the Supporting Information). Compound **1** was stable up to 180 °C, and then a rapid weight loss of ∼34% (exptl) was observed between 180 to 320 °C, which can be attributed to the loss of bpmh linkers (calcd = 39.8%) and then decomposes to an unidentified product. Compound **2** was found to be stable up to 260 °C; the first step weight loss of 31% (calcd = 37%) in the range of 260−350 °C could be due to the loss of the bpmh linker, and the second step weight loss of ∼40% (calcd = 44%) in the temperature range of 350−500 °C is due to the decomposition of the 1,3-adaa ligand, and the remaining organic ligands start burning above 500 °C. Compound **3** was stable up to 120 °C, and a weight loss of 45% was observed between 120 and 320 °C and then gradually decomposed in the temperature range of 320−500 °C, whereas compound **4**, also stable up to 120 °C, then started losing the 1,4-pdaa ligand, which was confirmed by 40% weight loss (calcd = 42%). The

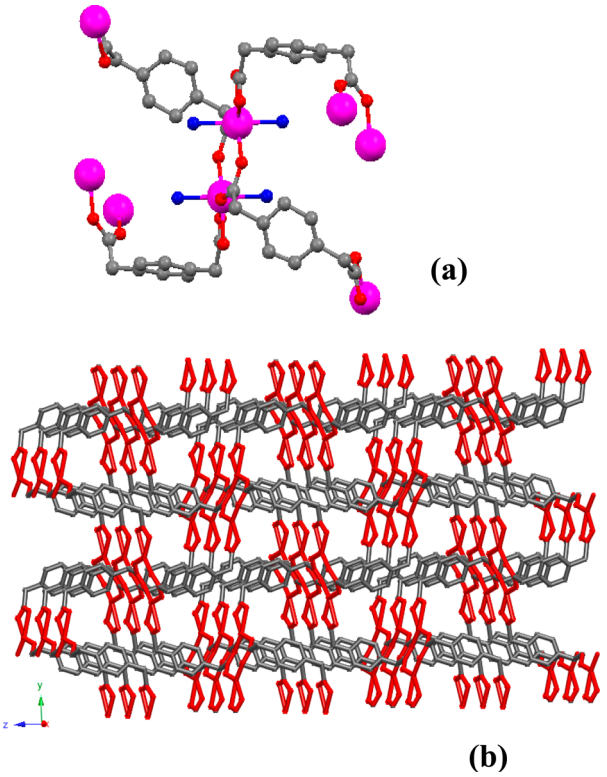

Figure 7. (a) 1,4-pdaa Ligand connectivity in the 3D framework. (b) 3D Framework of compounds **3** and **4** (bpmh linker has been omitted for clarity). Color code is the same as in Figure 6.

second step weight loss started at 270 °C probably due to decomposition.

Luminescence Properties. The ligand-based luminescence in MOF's is an attractive research topic for the selective sensing and detection of the metal ions.[21] Apart from the conventional applications, MOFs have been used as photoluminescent materials, owing to their higher stability compared to the organic materials and some typical advantages over inorganics.[22,7b] Generally, d^{10} complexes are promising to exhibit the photoluminescence properties.[23] We have investigated the solid-state emission properties of both the ligands as well as complexes **1** and **2** (Figure 8). The solid-state fluorescence maxima of 1,3-adaa and bpmh was observed at 406 and 403 nm excited at λ_{ex} = 280 nm, respectively (Figures

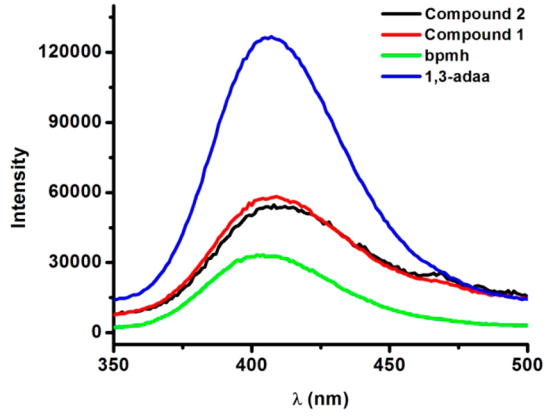

Figure 8. Solid-state fluorescence spectra of bpmh and 1,3-adaa ligands, as well as compounds **1** and **2**.

dx.doi.org/10.1021/cg401403a | *Cryst. Growth Des.* XXXX, XXX, XXX−XXX

S19 and S20 of the Supporting Information). The emission spectra of **1** and **2** resembles both ligands, but the intensity of both the complexes were different. Complexes **1** and **2** exhibit an emission band with a maxima at 406 nm for an excitation at λ_{ex} = 280 nm (Figures S21 and S22 of the Supporting Information). For d^{10} complexes, no emission originates from metal-centered MLCT/LMCT excited states, since the d^{10} metal ions are difficult to be oxidized or reduced.[24] Thus, the emission observed in the complexes is tentatively assigned to the ($n \rightarrow \pi^*$ and $\pi \rightarrow \pi^*$) intraligand fluorescence (i.e., ligand-based emission). The difference in the intensity of the emission band of compounds **1** and **2** from the ligands may be attributed to a different rigidity of the crystal packing in the solid state.[25] The slight differences in the positions of luminescent peaks in compounds **1** and **2** may be due to the different coordination modes of the ligands. It is surprising to note that there is no emission band observed for compound **3** on excitation in the range of 280 to 372 nm, although intense fluorescent emissions were observed for free ligands. [Fluorescence maxima was observed at 456 nm (λ_{ex} = 372 nm) for free 1,4-H_2pdaa and at 402 nm (λ_{ex} = 208 nm) for free bpmh]. Although the reason for the absence of the emission band for complex **3** was not clear, it might be attributed to the difference in the dicarboxylate ligand. Since in **1** and **2**, the 1,3-adaa ligand contains a rigid adamantane ring which, upon coordination [Zn(II) for **1** and Cd(II) for **2**, respectively], increases the rigidity of the ligand and reduces the loss of energy by radiationless decay, thereby enhancing the luminescence in comparison to **3**.[26] In compound **3**, the 1,4-pdaa ligand does not have such a type of rigid moiety, which might contribute to the absence of the luminescence.

Magnetic Properties. For magnetic investigation, dc susceptibility data was collected for compound **4** on the polycrystalline sample in the temperature range of 1.8−300 K at 0.1 T. The dc magnetic susceptibilities are shown in the form of the $\chi_M T$ (where χ_M is the molecular magnetic susceptibility) versus temperature (T) plot in Figure 9. The room temperature

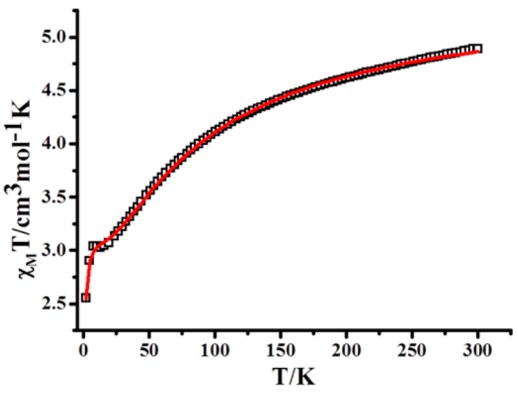

Figure 9. Temperature dependence of $X_M T$ collected in an applied field of 0.1 T for complex **4**. The red line represents the best fit obtained from the noncritical scaling theory.

$\chi_M T$ value of 4.88 cm^3 mol^{-1} K is higher than the expected spin-only value of 3.75 cm^3 mol^{-1} K (for 2 isolated Co^{2+}, g = 2.0) due to the orbital contribution to the magnetic moment. Once the temperature is lowered from 300 K, the $\chi_M T$ value decreases gradually, due to the antiferromagnetic interactions between metal centers and shows a plateaulike behavior between 20 to 10 K, probably owing to the spin−orbit coupling effect. With further decline of temperature, the $\chi_M T$ value decreases rapidly to reach the value of 2.55 cm^3 mol^{-1} K at 1.8 K. The decline at a low temperature is probably due to zero-field splitting.[14]

The magnetic susceptibility above 50 K nicely follow the Curie−Weiss law [$\chi_M T = C/(T - \theta)$], giving C = 5.3 cm^3 K mol^{-1} and θ = −29.6 K (Figure S23 of the Supporting Information). The negative value of θ indicates antiferromagnetic coupling between the Co(II) ions. To understand the low-temperature behavior, the experimental data (Figure 9) were fitted using the noncritical-scaling theory with the following simple phenomenological equation.[27]

$$\chi_M T = A \exp(-E_1/kT) + B \exp(-E_2/kT)$$

where $E_1 > 0$ represents the activation energies corresponding to the spin−orbit coupling, E_2 signifies the antiferromagnetic exchange interactions, and (A + B) equals the Curie constant. The best fit to the above equation was obtained with the fitting value of E_1/k = 0.38 cm^{-1}, E_2/k = 85.21 cm^{-1}, and (A + B) = 5.4 cm^3 K mol^{-1}. Obtained A + B values agrees well with the fitting of the Curie−Weiss equation at high temperature. The low E_1 value suggests little contribution of the spin−orbit coupling, and a high value of E_1 indicates significant antiferromagnetic exchange between adjacent Co^{2+} centers.

The $M/N\mu B$ verses H plots from 2 to 10 K (Figures S24 of the Supporting Information) show a steady increase with the field that reaches up to 3.44 μB at 7 T and 2 K, which is inconsistent with the expected value of 6 μB (for 2 isolated Co^{2+}, g = 2.0). This indicates the presence of antiferromagnetic interactions, even at the highest field of 7 T. The $M/N\mu B$ verses the H/T plot (Figure S25 of the Supporting Information) further confirms the presence of the little anisotropy of Co^{2+} centers, which prevents single molecular magnetic behavior from being shown.

CONCLUSION

In this work, we have reported a family of four 2D/3D MOFs prepared using a neutral, long, and rigid bis-pyridyl ligand and two dicarboxylates. Compounds **1** and **2** reveal ligand-based photoluminescence properties in the solid state. The magnetic properties of compound **4** show antiferromagnetic behavior among the metal centers. We are currently working with this neutral ligand to explore the possibility of it providing large pore sizes, a high surface area, and much required additional stability to the MOFs.

ASSOCIATED CONTENT

Supporting Information

Synthetic procedure for bpmh ligand, PXRD patterns of compounds **1**−**4**, TGA, IR data, CIF files, and additional figures. This material is available free of charge via the Internet at http://pubs.acs.org.

AUTHOR INFORMATION

Corresponding Author

*E-mail: skonar@iiserb.ac.in.

Author Contributions

‡These authors equally contributed to this work.

Notes

The authors declare no competing financial interest.

■ ACKNOWLEDGMENTS

S.S. and S.P. thank IISER Bhopal for the Ph.D. fellowships. A.A. thanks CSIR for the SRF fellowship. The authors thank Dr. H. S. Jena for helpful scientific discussions. S.K. thanks CSIR, Government of India (Project No.01/(2473)/11/EMRII), and IISER Bhopal for generous financial and infrastructural support.

■ REFERENCES

(1) (a) Koh, K.; Wong-Foy, A. G.; Matzger, A. J. *J. Am. Chem. Soc.* **2009**, *131*, 4184−4185. (b) Farha, O. K.; Eryazici, I.; Jeong, N. C.; Hauser, B. G.; Wilmer, C. E.; Sarjeant, A. A.; Snurr, R. Q.; Nguyen, S. T.; Yazaydın, A. O.; Hupp, J. T. *J. Am. Chem. Soc.* **2012**, *134*, 15016−15021. (c) Furukawa, H.; Ko, N.; Go, Y. B.; Aratani, N.; Choi, S. B.; Choi, E.; Yazaydın, A. Ö.; Snurr, R. Q.; O'Keeffe, M.; Kim, J.; Yaghi, O. M. *Science* **2010**, *329*, 424−428. (d) Farha, O. K.; Yazaydın, A. Ö.; Eryazici, I.; Malliakas, C. D.; Hauser, B. G.; Kanatzidis, M. G.; Nguyen, S. T.; Snurr, R. Q.; Hupp, J. T. *Nat. Chem.* **2010**, *2*, 944−948.

(2) (a) Morris, W.; Volosskiy, B.; Demir, S.; Gándara, F.; Mc Grier, P. L.; Furukawa, H.; Cascio, D.; Stoddart, J. F.; Yaghi, O. M. *Inorg. Chem.* **2012**, *51*, 6443−6445. (b) Park, H. J.; Lim, D. W.; Yang, W. S.; Oh, T. R.; Suh, M. P. *Chem.−Eur. J.* **2011**, *17*, 7251−7260. (c) Shultz, A. M.; Farha, O. K.; Hupp, J. T.; Nguyen, S. T. *J. Am. Chem. Soc.* **2009**, *131*, 4204−4205. (d) Makal, T. A.; Li, J. R.; Lu, W.; Zhou, H. C. *Chem. Soc. Rev.* **2012**, *41*, 7761−7779.

(3) (a) Chen, B.; Wang, L.; Zapata, F.; Qian, G.; Lobkovsky, E. B. *J. Am. Chem. Soc.* **2008**, *130*, 6718−6719. (b) Chen, B.; Wang, L.; Xiao, Y.; Fronczek, F. R.; Xue, M.; Cui, Y.; Qian, G. *Angew. Chem., Int. Ed.* **2009**, *48*, 500−503. (c) Rieter, W. J.; Taylor, K. M. L.; Lin, W. *J. Am. Chem. Soc.* **2007**, *129*, 9852−9853.

(4) (a) Ma, L.; Abney, C.; Lin, W. *Chem. Soc. Rev.* **2009**, *38*, 1248−1256. (b) Dybtsev, D. N.; Nuzhdin, A. L.; Chun, H.; Bryliakov, K. P.; Talsi, E. P.; Fedin, V. P.; Kim, K. *Angew. Chem., Int. Ed.* **2006**, *45*, 916−920. (c) Cho, S. H.; Ma, B.; Nguyen, S. T.; Hupp, J. T.; Albrecht-Schmittb, T. E. *Chem. Commun.* **2006**, 2563−2565.

(5) (a) Rao, C. N. R.; Cheetham, A. K.; Thirumurugan, A. *J. Phys.: Condens. Matter* **2008**, *20*, 083202. (b) Chakraborty, A.; Ghosh, B. K.; Arino, J. B.; Ribas, J.; Maji, T. K. *Inorg. Chem.* **2012**, *51*, 6440−6442. (c) Kurmoo, M. *Chem. Soc. Rev.* **2009**, *38*, 1353−1379 and reference cited therein. (d) Halder, G. J.; Kepert, C. J.; Moubaraki, B.; Murray, K. S.; Cashion, J. D. *Science* **2002**, *298*, 1762−1765.

(6) (a) Farha, O. K.; Hupp, J. T. *Acc. Chem. Res.* **2010**, *43*, 1166−1175. (b) Horcajada, P.; Serre, C.; Vallet-Regi, M.; Sebban, M.; Taulelle, F.; Ferey, G. *Angew. Chem., Int. Ed.* **2006**, *45*, 5974−5978. (c) Rocca, J. D.; Liu, D.; Lin, W. *Acc. Chem. Res.* **2011**, *44*, 957−968 and references cited there in.

(7) (a) Lu, G.; Hupp, J. T. *J. Am. Chem. Soc.* **2010**, *132*, 7832−7833. (b) Kreno, L. E.; Leong, K.; Farha, O. K.; Allendorf, M.; Van Duyne, R. P.; Hupp, J. T. *Chem. Rev.* **2012**, *112*, 1105−1125 and references cited therein.

(8) (a) D'Andrade, B. W.; Forrest, S. R. *Adv. Mater.* **2004**, *16*, 1585−1595. (b) Cui, Y.; Yue, Y.; Qian, G.; Chen, B. *Chem. Rev.* **2012**, *112*, 1126−1162 and references cited therein.

(9) (a) Nagarkar, S. S.; Joarder, B.; Chaudhari, A. K.; Mukherjee, S.; Ghosh, S. K. *Angew. Chem., Int. Ed.* **2013**, *52*, 2881−2885. (b) Lan, A.; Li, K.; Wu, H.; Olson, D. H.; Emge, T. J.; Ki, W.; Hong, M.; Li, J. *Angew. Chem., Int. Ed.* **2009**, *48*, 2334−2338. (c) Pramanik, S.; Zheng, C.; Zhang, X.; Emge, T. J.; Li, J. *J. Am. Chem. Soc.* **2011**, *133*, 4153−4155.

(10) (a) Tranchemontagne, D. J.; Mendoza-Cortés, J. L.; O'Keeffe, M.; Yaghi, O. M. *Chem. Soc. Rev.* **2009**, *38*, 1257−1283. (b) Natarajan, S.; Mahata, P. *Chem. Soc. Rev.* **2009**, *38*, 2304−2318.

(11) (a) Wang, F.; Jing, X.; Zheng, B.; Li, G.; Zeng, G.; Huo, Q.; Liu, Y. *Cryst. Growth Des.* **2013**, *13*, 3522−3527. (b) Huang, R. W.; Zhu, Y.; Zang, S. Q.; Zhang, M. L. *Inorg. Chem. Commun.* **2013**, *33*, 38−42. (c) Qi, M. L.; Yu, K.; Su, Z. H.; Wang, C. X.; Wang, C. M.; Zhou, B. B.; Zhu, C. C. *Dalton Trans.* **2013**, *42*, 7586−7594.

(12) (a) Liu, G. L.; Qin, Y. J.; Jing, L.; Wei, G. Y.; Li, H. *Chem. Commun.* **2013**, *49*, 1699−1701. (b) Zhao, S. N.; Su, S. Q.; Song, X. Z.; Zhu, M.; Hao, Z. M.; Meng, X.; Song, S. Y.; Zhang, H. J. *Cryst. Growth Des.* **2013**, *13*, 2756−2765. (c) Han, Q.; He, C.; Zhao, M.; Qi, B.; Niu, J.; Duan, C. *J. Am. Chem. Soc.* **2013**, *135*, 10186−10189. (d) Hazra, A.; Bonakala, S.; Reddy, S. K.; Balasubramanian, S.; Maji, T. K. *Inorg. Chem.* **2013**, *52*, 11385−11397. (e) Kettner, F.; Worch, C.; Moellmer, J.; Gläser, R.; Staudt, R.; Krautscheid, H. *Inorg. Chem.* **2013**, *52*, 8738−8742.

(13) (a) Gai, Y. L.; Jiang, F. L.; Xiong, K. C.; Chen, L.; Yuan, D. Q.; Zhang, L. J.; Zhou, K.; Hong, M. C. *Cryst. Growth Des.* **2012**, *12*, 2079−2088. (b) Déniz, M.; Rodríguez, I. H.; Pasán, J.; Fabelo, O.; Delgado, L. C.; Yuste, C.; Julve, M.; Lloret, F.; Ruiz-Pérez, C. *Cryst. Growth Des.* **2012**, *12*, 4505−4518. (c) Bury, W.; Jimenez, D. F.; Lalonde, M, B.; Snurr, R. Q.; Farha, O. K.; Hupp, J. T. *Chem. Mater.* **2013**, *25*, 739−744. (d) Karagiaridi, O.; Bury, W.; Tylianakis, E.; Sarjeant, A. A.; Hupp, J. T.; Farha, O. K. *Chem. Mater.* **2013**, *25*, 3499−3503.

(14) Kahn, O. *Molecular Magnetism*; VCH: New York, 1993.

(15) Sheldrick, G. M. *SHELXTL, Program for the Solution of Crystal of Structures*; University of Göttingen: Göttingen, Germany, 1993.

(16) Sheldrick, G. M. *SHELXL 97, Program for Crystal Structure Refinement*; University of Göttingen: Göttingen, Germany, 1997.

(17) Spek, A. L. *J. Appl. Crystallogr.* **2003**, *36*, 7.

(18) Farrugia, L. J. *J. Appl. Crystallogr.* **1999**, *32*, 837.

(19) Kennedy, A. R.; Brown, K. G.; Graham, D.; Kirkhouse, J. B.; Kittner, M.; Major, C.; McHugh, C. J.; Murdoch, P.; Smith, W. E. *New J. Chem.* **2005**, *26*, 826−832.

(20) (a) Zhang, S. Q.; Jiang, F. L.; Wu, M .Y.; Ma, J.; Bu, Y.; Hong, M. C. *Cryst. Growth Des.* **2012**, *12*, 1452−1463. (b) Su, S.; Qin, C.; Guo, Z.; Guo, H.; Song, S.; Deng, R.; Cao, F.; Wang, S.; Lic, G.; Zhang, H. *CrystEngComm* **2011**, *13*, 2935−2941. (c) Amiri, M. G.; Mahmoudi, G.; Morsali, A.; Hunterb, A. D.; Zeller, M. *CrystEngComm* **2007**, *9*, 686−697. (d) Yang, W.; Lin, X.; Blake, A. J.; Wilson, C.; Hubberstey, P.; Champness, N. R.; Schröder, M. *Inorg. Chem.* **2009**, *48*, 11067−11078. (e) Dey, R.; Haldar, R.; Maji, T. K.; Ghoshal, D. *Cryst. Growth Des.* **2011**, *11*, 3905−3911. (f) Drabent, K.; Ciunik, Z. *Cryst. Growth Des.* **2009**, *9*, 3367−3375. (g) Granifo, J.; Garland, M. T.; Baggio, R. *Polyhedron* **2006**, *25*, 2277−2283. (h) Mahmoudi, G.; Morsali, A.; Zeller, M. *Inorg. Chim. Acta* **2009**, *362*, 217−225. (i) Shoshnik, R.; Elengoz, H.; Goldberg, I. *Acta Crystallogr., Sect. C* **2005**, *61*, m187−m189.

(21) (a) Paz, F. A. A.; Klinowski, J.; Vilela, S. M. F.; Tome, J. P. C.; Cavaleiroc, J. A. S.; Rocha, J. *Chem. Soc. Rev.* **2012**, *41*, 1088−1110. (b) Doty, F. P.; Bauer, C. A.; Skulan, A. J.; Grant, P. G.; Allendorf, M .D. *Adv. Mater.* **2009**, *21*, 95−101. (c) Takashima, Y.; Martinez, V. M.; Furukawa, S.; Kondo, M.; Shimomura, S.; Uehara, H.; Nakahama, M.; Sugimoto, K.; Kitagawa, S. *Nat. Commun.* **2011**, *2*, 1618.

(22) He, K. H.; Song, W. C.; Li, Y. W.; Chen, Y. Q.; Bu, X. H. *Cryst. Growth Des.* **2012**, *12*, 1064−1068.

(23) (a) Fang, H. C.; Zhu, J. Q.; Zhou, L. J.; Jia, H. Y.; Li, S. S.; Gong, X.; Li, S. B.; Cai, Y. P.; Thallapally, P. K.; Liu, J.; Exarhos, G. J. *Cryst. Growth Des.* **2010**, *10*, 3277−3284. (b) Dai, J. C.; Wu, X. T.; Fu, Z. Y.; Cui, C. P.; Hu, S. M.; Du, W. X.; Wu, L. M.; Zhang, H. H.; Sun, R. Q. *Inorg. Chem.* **2002**, *41*, 1391−1396. (c) Zheng, S. L.; Yang, J. H.; Yu, X. L.; Chen, X. M.; Wong, W. T. *Inorg. Chem.* **2004**, *43*, 830−838. (d) Zang, S. Q.; Cao, L. H.; Liang, R.; Hou, H. W.; Mak, T. C. W. *Cryst. Growth Des.* **2012**, *12*, 1830−1837. (e) Liang, X. Q.; Zhou, X. H.; Chen, C.; Xiao, H. P.; Li, Y. Z.; Zuo, J. L.; You, X. Z. *Cryst. Growth Des.* **2009**, *9*, 1041−1053. (f) Niu, D.; Yang, J.; Guo, J.; Kan, W. Q.; Song, S. Y.; Du, P.; Ma, J. F. *Cryst. Growth Des.* **2012**, *12*, 2397−2410.

(24) (a) Liu, H. Y.; Wu, H.; Ma, J. F.; Liu, Y. Y.; Liu, B.; Yang, J. *Cryst. Growth Des.* **2010**, *10*, 4795−4805. (b) Zhang, L. P.; Ma, J. F.; Yang, J.; Pang, Y. Y.; Ma, J. C. *Inorg. Chem.* **2010**, *49*, 1535−1550. (c) Wen, L.; Lu, Z.; Lin, J.; Tian, Z.; Zhu, H.; Meng, Q. *Cryst. Growth Des.* **2007**, *7*, 93−99. (d) Bai, H. Y.; Ma, J. F.; Yang, J.; Liu, Y. Y.; Wu, H.; Ma, J. C. *Cryst. Growth Des.* **2010**, *10*, 995−1016.

(25) (a) Zhang, L. Y.; Liu, G. F.; Zheng, S. L.; Ye, B. H.; Zhang, X. M.; Chen, X. M. *Eur. J. Inorg. Chem.* **2003**, 2965−2971. (b) *Photochemistry and Photophysics of Coordination Compounds*; Yersin, H.; Vogler, A., Eds.; Springer: Berlin, 1987.

(26) (a) Lan, Y. Q.; Li, S. L.; Qin, J. S.; Du, D. Y.; Wang, X. L.; Su, Z. M.; Fu, Q. *Inorg. Chem.* **2008**, *47*, 10600−10610. (b) Li, S. L.; Lan, Y. Q.; Ma, J. F.; Yang, J.; Wei, G. H.; Zhang, L. P.; Su, Z. M. *Cryst. Growth Des.* **2008**, *8*, 675−684. (c) Li, S. L.; Lan, Y. Q.; Ma, J. F.; Fu, Y. M.; Yang, J.; Ping, G. J.; Liu, J.; Su, Z. M. *Cryst. Growth Des.* **2008**, *8*, 1610−1616. (d) Ren, C.; Zhang, Y. N.; Shi, W. J.; Liu, B.; Wang, Y. Y.; Shi, Q. Z. *CrystEngComm* **2011**, *13*, 5179−5189.

(27) (a) Zeng, M. H.; Zhou, Y. L.; Wu, M. C.; Sun, H. L.; Du, M. *Inorg. Chem.* **2010**, *49*, 6436−6442. (b) Miller, J. S.; Drillon, M. *Magnetism: Molecule to Materials V*; Wiley-VCH: Weinheim, Germany, 2005; pp347; (c) Yao, R. X.; Qin, Y. L.; Ji, F.; Zhao, Y. F.; Zhang, X. M. *Dalton Trans.* **2013**, *42*, 6611−6618.